Electronic Supplementary Material (ESI) for Inorganic Chemistry Frontiers.

Supporting Information

Solvatochromic dual luminescence of Eu-Au dyads decorated with chromophore phosphines

Andrey Belyaev,[a] Sofia O. Slavova,[bc] Igor V. Solovyev,[b] Vladimir Sizov,[b] Janne Jänis,[a] Elena V. Grachova,[b] Igor O. Koshevoy[a]**

[a] Department of Chemistry, University of Eastern Finland, Joensuu, 80101, Finland

[b] Institute of Chemistry, St. Petersburg State University, St. Petersburg, 198504, Russia

[c] Institute of General and Inorganic Chemistry, Bulgarian Academy of Sciences, Sofia, 1113, Bulgaria

E-mail: e.grachova@spbu.ru; igor.koshevoy@uef.fi

Table of Contents

Experimental section

General comments. 4-(*N,N*-diphenylamino)-4'-bromobiphenyl,[1] 4-ethynyl-*N,N*-diphenylaniline,[2] 9,10-dibromoanthracene[3] $[Au(epbpy)]_n$ (epbpy = 5-(4-ethynylphenyl)-2,2′-bipyridine),[4] $Eu(tta)_3 \times 2H_2O$ (tta = 3-thenoyltrifluoroacetonate),[5] were synthesized according to the published procedures. Tetrahydrofuran (THF), toluene and diethyl ether were distilled over Na-benzophenone ketyl under a nitrogen atmosphere prior to use. The syntheses of the phosphine ligands **L1**–**L3** and of their precursors was carried out under a nitrogen atmosphere. Other reagents and solvents were used as received. The solution on ^1H, $^{31}P\{^1H\}$ and ^1H–^1H COSY NMR spectra were recorded on Bruker Avance 400 and AMX-400 spectrometers. Mass spectra were recorded on a Bruker Solarix XR instrument in the ESI^+ and APPI (atmospheric pressure photoionization) modes. The infrared (FTIR) spectra were measured on a Bruker VERTEX 70 FT-IR spectrometer. Microanalyses were carried out in the analytical laboratory of the University of Eastern Finland using vario MICRO cube CHNS-analyzer (Elementar, Germany).

Computational details. The long-range-corrected LC-PBE functional was used for geometry optimization of all studied compounds.[6-7] When calculating the absorption spectra, the hybrid functional CAM-B3LYP,[8] which adequately describes the complexes with charge transfer. For Eu(III), a large-core version of the Stuttgart-Dresden MWB potential was selected as the basis set, which does not consider f-electrons explicitly, but includes them in the composition of the core.[9] This approach simplifies the calculations and significantly improves SCF convergence in comparison with the large-core version, reduces the estimated time without affecting the quality of the calculated design characteristics. The standard version of the MWB60 potential was used for Au(I), and 6-31G * basis set was used for all other atoms. Where appropriate, solvent effects were taken into account using the IEF-PCM formalism.[10-11] Solvent-dependent luminescent properties of **Au1**–**Au3** were studied in the framework of state-specific solvation approach.[12] The nature of the excited states was analyzed by natural transition orbitals (NTO) formalism.[13] All quantum chemical calculations were performed by using the software package Gaussian 16.[14]

Photophysical measurements. The photophysical measurements in solution were carried out at concentration of *ca*. $1\text{-}5\times10^{-5}$ M (10 mm cuvettes) in cyclohexane (CHX), toluene, dichloromethane (DCM), 1,2-dichloroethane, chloroform ($CHCl_3$), diethyl ether (Et_2O), tetrahydrofuran (THF), acetone and acetonitrile (MeCN), which were distilled prior to use. Steady-state absorption spectra were recorded using a PerkinElmer Lambda 900 UV/VIS/NIR and Shimadzu UV-1800 spectrophotometers. The excitation and photoluminescence spectra were collected on a HORIBA FluoroMax-4, Fluorolog-3 and AVANTES AvaSpec-ULS4096CL-EVO

spectrofluorimeters. The Xe lamps (300 W and 450 W) and LED 365 nm was used as an excitation light source to obtain luminescence. Lifetimes were determined by the time-correlated single photon counting (TCSPC) method using a HORIBA Fluorolog-3 spectrofluorimeter and photon-counting system with a LED (maximum of emission at 340 nm) in pulse mode (width 0.9 nm, repetition rate 100 kHz) for nanosecond domain or Xe lamp (450 W, repetition rate 10 kHz) for microsecond domain as the excitation source. The lifetime data were fitted using the HORIBA Instruments software package and the Origin 9.55b program. The relative emission quantum yield in solution was determined by the comparative method.[15] Coumarine-102 (in ethanol, $\Phi_{em} = 0.764$) and rhodamine 6G (in water, $\Phi_{em} = 0.962$) was used as a reference standard.

Solvent-variable optical characteristics for **Au1**−**Au3** were analyzed using the Lippert−Mataga equation, which describes the dependence of the Stokes shift between the absorption and emission bands (ν_{St}, cm^{-1}) on the solvent polarity parameter (Δf):[16-17]

$$\nu_{St} = \frac{2(\Delta\mu)^2\ \Delta f}{4\pi\varepsilon_0\ hca_0^3} + const$$

$\Delta\mu = \mu_{es} - \mu_{gs}$ (D) is the difference between the dipole moments in the excited and the ground states, ε_0 is the permittivity of vacuum (8.85×10^{-12} $C^2\ J^{-1}\ m^{-1}$), h is Planck's constant (6.63×10^{-34} J s), c is the velocity of light (3×10^{10} cm s^{-1}), a_0 is the radius of the Onsager cavity around the fluorophore (m). The Onsager radii for metalloligands were estimated from the DFT optimized structures (7.7 Å for **Au1**, 9.1 Å for **Au2** and 10.1 Å for **Au3**) as half of the distance between diphenylamine donor and the acceptor diphenylphosphine groups, which corresponds to the part of the molecule where charge separation takes place; Δf is the orientation polarizability (intrinsic solvent polarity), which is determined by the corresponding dielectric constant (ε) and refractive index (n):

$$\Delta f = \frac{\varepsilon - 1}{2\varepsilon + 1} - \frac{n^2 - 1}{2n^2 + 1}$$

Commission internationale de l'éclairage (CIE 1931) coordinates was calculated from photoluminescence data by using Origin 9.55b software pack.

Syntheses

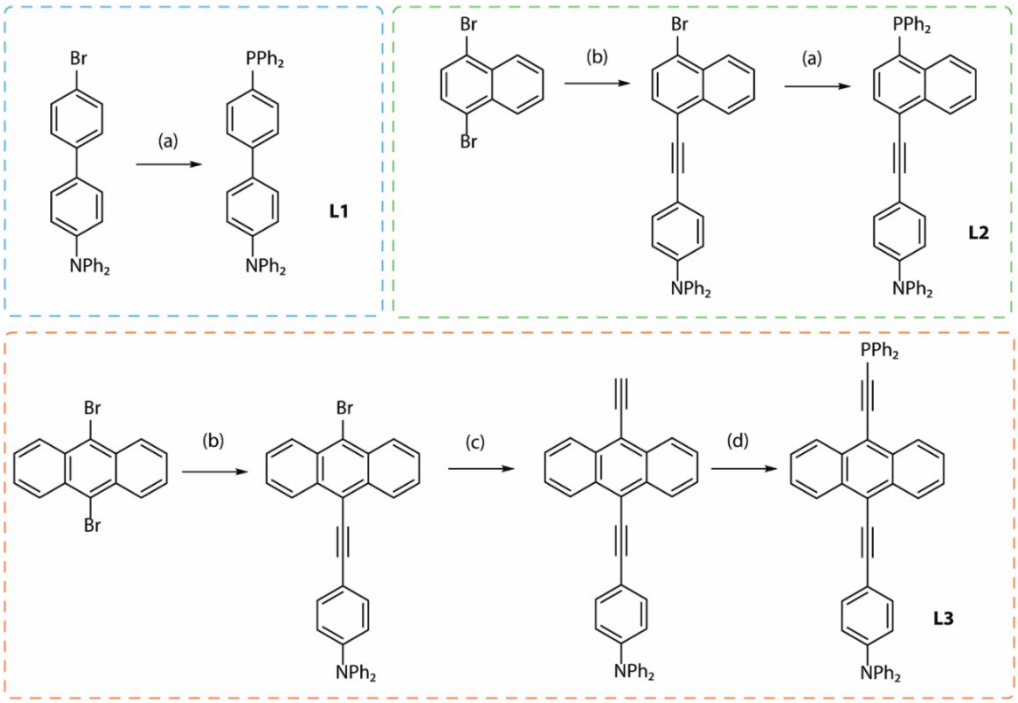

Scheme S1. Synthetic routes to achieve ligands **L1**–**L3**: (**a**) *i*. *n*-BuLi 2.5 M, THF, –78 °C, 1 h; *ii*. PPh_2Cl, –78 °C → rt, 2h; (**b**) *p*-$HC_2C_6H_4NPh_2$, $Pd(PPh_3)_2Cl_2$, PPh_3, CuI, i-Pr_2NH/THF (1/1), 60 °C, 10h; (**c**) *i*. HC_2SiMe_3, $Pd(PPh_3)_2Cl_2$, PPh_3, CuI, i-Pr_2NH/THF (1/1), 60 °C, 10h; *ii*. KOH, methanol/THF (1/2), rt, 1h; (**d**) *i*. *n*-BuLi 1.6 M, diethyl ether/THF (1/1) –85 °C, 1 h; *ii*. PPh_2Cl, –78 °C → rt, 2h.

4-(Diphenylphosphino)-4´-(*N,N*-diphenylamino)-biphenyl (L1).[18] A solution of 4-(*N,N*-diphenylamino)-4'-bromobiphenyl (2.00 g, 5.0 mmol) in THF (40 ml) was cooled to –78 °C, and a 1.6 M solution of *n*-BuLi in hexane (3.4 mL, 5.4 mmol) was added dropwise within 10 min. to give a light yellow clear solution, which was stirred at this temperature for 1 h, and then it was treated dropwise with neat PPh_2Cl (1.2 g, 5.4 mmol). The reaction mixture was allowed to reach room temperature and was stirred for additional 1 h. Then it was quenched with methanol (2 ml) and evaporated. The solid residue was washed with deaerated methanol (3 × 15 ml) and dried. Crude **L1** was purified by column chromatography (Silica gel 70–230 mesh, 2.5×15 cm, eluent dichloromethane-hexane 2:3 v/v). The solvents were evaporated to afford nearly colourless foam-like amorphous solid, which was additionally digested with air-free methanol (15 ml) and dried (1.96 g, 78 %). $^{31}P\{^1H\}$ NMR (CD_2Cl_2; 298 K; δ): –6.9 (s, 1P, PPh_2).

^{1}H NMR (CD_2Cl_2, 298 K; δ): 7.56 (dd, 2H, J_{HH} 8.4 and 1.4 Hz), 7.49 (d, 2H, J_{HH} 8.8 Hz), 7.38–7.31 (m, 12H), 7.28 (dd, 4H, J_{HH} 8.5 and 7.3 Hz), 7.13–7.08 (m, 6H), 7.05 (tt, 2H, J_{HH} 7.3 and 1.2 Hz).

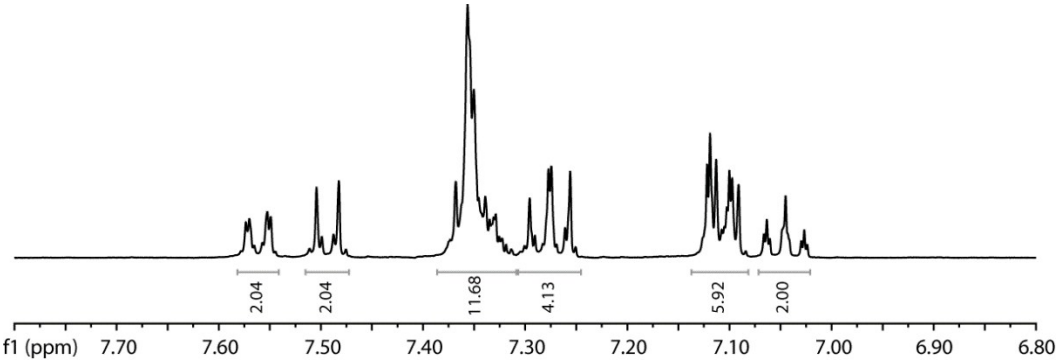

Anal. Calc. for $C_{36}H_{28}NP$: C, 85.52; H, 5.58; N, 2.77. Found: C 85.06; H 5.26; N, 2.38.

4-[(4-Bromonaphthalen-1-yl)ethynyl]-*N,N*-diphenylaniline. A mixture of 1,4-dibromonaphthalene (1.90 g, 5.6 mmol), 4-ethynyl-*N,N*-diphenylaniline (1.37 g, 5.1 mmol), $Pd(PPh_3)_2Cl_2$ (0.36 g, 0.5 mmol), PPh_3 (0.13 g, 0.5 mmol) and CuI (0.10 g, 0.5 mmol) in *i*-Pr_2NH/THF 1:1 v/v mixture (70 ml) was stirred at 60 °C for 10 h under a nitrogen atmosphere. Then the reaction mixture was poured into water (150 ml) and extracted with dichloromethane (3×50 ml). Combined organic layers were dried over anhydrous Na_2SO_4, filtered and evaporated. The resulting brown oil was purified by column chromatography (Silica gel 70–230 mesh, 4×20 cm, eluent dichloromethane-hexane, 1:7 v/v) and further recrystallized from hot hexane to afford yellow crystalline material (1.40 g, 63 %). ^{1}H NMR ($CDCl_3$, 298 K; δ): 8.45–8.47 (m, 1H, naphthalene), 8.27–8.29 (m, 1H, naphthalene), 7.77 (d, 1H, J_{HH} 7.7 Hz, naphthalene), 7.64–7.66 (m, 2H, naphthalene), 7.58 (d, 1H, J_{HH} 7.7 Hz, naphthalene), 7.50 (d, 2H, J_{HH} 8.1 Hz, C_6H_4), 7.31 (dd, 4H, J_{HH} ca. 7.6 Hz, *meta*-H NPh_2), 7.16 (d, 4H, J_{HH} 7.6 Hz, *ortho*-H NPh_2), 7.06–7.12 (m, 4H, *para*-H NPh_2 + C_6H_4). Anal. Calc. for $C_{30}H_{20}BrN$: C, 75.96; H, 4.25; N, 2.95. Found: C 76.01; H 4.12; N, 3.11.

4-[(4-(Diphenylphosphaneyl)naphthalen-1-yl)ethynyl]-*N,N*-diphenylaniline (L2). Prepared analogously to **L1** from 4-[(4-bromonaphthalen-1-yl)ethynyl]-*N,N*-diphenylaniline (1.00 g, 2.1 mmol), *n*-BuLi (2.5 M in hexanes, 0.9 mL, 2.3 mmol) and PPh_2Cl (0.46 g, 2.1 mmol). The resulting yellow solid residue was washed with methanol (4×15 ml) and diethyl ether (2×10 ml) and dried. Crude **L3** was passed through a pad of Silica gel (70–230 mesh, 3×6 cm, eluent dichloromethane-hexane, 1:1 v/v) and dried *in vacuo* to afford bright yellow solid (0.59 g, 49 %). $^{31}P\{^1H\}$ NMR ($CDCl_3$; 298 K; δ): –14.1 (s, 1P, PPh_2). ^{1}H NMR ($CDCl_3$, 298 K; δ): 8.49 (m, 1H, naphthalene), 8.42–8.45 (m, 1H, naphthalene), 7.56–7.60 (m, 2H, naphthalene), 7.46–7.51 (m, 3H, naphthalene + C_6H_4), 7.29–7.37 (m, 14H, PPh_2 + *meta*-H NPh_2), 7.14 (d, 4H, J_{HH} 7.6 Hz, *ortho*-H NPh_2), 7.04–

7.10 (m, 4H, *para*-H NPh_2 + C_6H_4), 6.96 (dd, 1H, J_{HH} 7.4, 4.7 Hz, naphthalene). Anal. Calc. for $C_{42}H_{30}NP$: C, 87.02; H, 5.22; N, 2.42. Found: C 86.65; H 5.00; N, 2.31.

4-[(10-Bromoanthracen-9-yl)ethynyl]-*N,N*-diphenylaniline. Prepared analogously to 4-[(4-bromonaphthalen-1-yl)ethynyl]-*N,N*-diphenylaniline from 9,10-dibromoanthracene (2.60 g, 7.8 mmol), 4-ethynyl-*N,N*-diphenylaniline (2.00 g, 7.4 mmol), $Pd(PPh_3)_2Cl_2$ (0.52 g, 0.7 mmol), PPh_3 (0.19 g, 0.7 mmol), CuI (0.14 g, 0.7 mmol) in *i*-Pr_2NH/THF 1:1.5 v/v mixture (125 ml). The resulting orange solid was purified by column chromatography (Silica gel 70-230 mesh, 4×20 cm, eluent dichloromethane-hexane, 1:5 v/v) to afford yellow-greenish product (2.15 g, 55 %). ^{1}H NMR ($CDCl_3$, 298 K; δ): 8.70–8.71 (m, 2H, anthracene), 8.57–8.59 (m, 2H, anthracene), 7.61–7.67 (m, 6H, anthracene + C_6H_4), 7.33 (dd, 4H, J_{HH} ca. 7.6 Hz, *meta*-H NPh_2), 7.19 (d, 4H, J_{HH} 7.6 Hz, *ortho*-H NPh_2), 7.09–7.13 (m, 4H, *para*-H NPh_2 + C_6H_4). Anal. Calc. for $C_{34}H_{22}BrN$: C, 77.87; H, 4.23; N, 2.67. Found: C 77.90; H 4.17; N, 2.77.

4-[(10-Ethynylanthracen-9-yl)ethynyl]-*N,N*-diphenylaniline. *i*. The synthesis was carried out under a nitrogen atmosphere. Trimethylsilylacetylene (0.60 g, 5.8 mmol) was added to a mixture of 4-[(10-bromoanthracen-9-yl)ethynyl]-*N,N*-diphenylaniline (2.00 g, 3.8 mmol), $Pd(PPh_3)_2Cl_2$ (0.28 g, 0.4 mmol), PPh_3 (0.10 g, 0.4 mmol) and CuI (0.08 g, 0.4 mmol) in *i*-Pr_2NH/THF 1:1 v/v mixture (100 ml) and reaction mixture was refluxed for 10 h. Then it was poured in water (150 ml) and extracted with dichloromethane (5×30 ml). Combined organic layers were dried over anhydrous Na_2SO_4, filtered and evaporated. The resulting orange solid was purified by column chromatography (Silica gel 70-230 mesh, 4×20 cm, eluent dichloromethane-hexane, 1:5 v/v) to afford orange microcrystalline material (1.28 g, 62 %). ^{1}H NMR ($CDCl_3$, 298 K; δ): 8.67–8.69 (m, 2H, anthracene), 8.60–8.62 (m, 2H, anthracene), 7.62–7.65 (m, 6H, anthracene + C_6H_4), 7.33 (dd, 4H, J_{HH} ca. 7.7 Hz, *meta*-H NPh_2), 7.18 (d, 4H, J_{HH} 7.7 Hz, *ortho*-H NPh_2), 7.10–7.13 (m, 4H, *para*-H NPh_2 + C_6H_4), 0.45 (s, 9H, Me).

ii. The obtained product was dissolved in methanol/THF 1:2 v/v mixture (60 ml) under a nitrogen atmosphere and KOH (0.27 g, 4.8 mmol) was added. The reaction mixture was stirred at room temperature for 1 h, then it was poured into water (200 ml) and extracted with dichloromethane (4×50 ml). Combined organic layers were dried over anhydrous Na_2SO_4, filtered and evaporated. The resulting orange solid was purified by column chromatography (Silica gel 70–230 mesh, 4×20 cm, eluent dichloromethane-hexane, 1:2 v/v) to afford orange microcrystalline material (0.88 g, 78 %). ^{1}H NMR ($CDCl_3$, 298 K; δ): 8.68–8.70 (m, 2H, anthracene), 8.61–8.64 (m, 2H, anthracene), 7.62–7.65 (m, 6H, anthracene + C_6H_4), 7.33 (dd, 4H, J_{HH} 8.0, 7.8 Hz, *meta*-H NPh_2), 7.18 (d, 4H, J_{HH} 8.0 Hz, *ortho*-H NPh_2), 7.09–7.13 (m, 4H, *para*-H NPh_2 + C_6H_4), 3.34 (s, 1H, C_2H). Anal. Calc. for $C_{36}H_{23}N$: C, 92.08; H, 4.94; N, 2.98. Found: C 91.45; H 4.66; N, 2.39.

4-[(10-((diphenylphosphaneyl)ethynyl)anthracen-9-yl)ethynyl]-*N*,*N*-diphenylaniline (L3). A solution of 4-[(10-ethynylanthracen-9-yl)ethynyl]-*N,N*-diphenylaniline (0.88 g, 1.9 mmol) in diethyl ether/THF 1:1 v/v mixture (80 ml) was cooled to –85 °C, and a 1.6 M solution of *n*-BuLi in hexane (1.3 mL, 2.1 mmol) was added dropwise within 10 min. to give a red suspension. The resulting mixture was stirred at this temperature for 1 h, then it was treated dropwise with neat PPh_2Cl (0.42 g, 1.9 mmol). The reaction mixture was allowed to reach room temperature and was stirred for additional 1 h, quenched with methanol (10 ml) and evaporated. The solid residue was washed with methanol (3×15 ml), dried and the crude material was passed through a pad of Silica gel (70–230 mesh, 3×6 cm, eluent dichloromethane) to afford red-brown product (0.65 g, 52 %). $^{31}P\{^1H\}$ NMR ($CDCl_3$; 298 K; δ): –32.8 (s, 1P, PPh_2). ^1H NMR ($CDCl_3$, 298 K; *δ*): 8.64–8.66 (m, 2H, anthracene), 8.52–8.55 (m, 2H, anthracene), 7.78–7.83 (m, 4H, *ortho*-H PPh_2), 7.54–7.61 (m, 6H, anthracene + C_6H_4), 7.38–7.43 (m, 6H, *meta*+*para*-H PPh_2), 7.33 (dd, 4H, J_{HH} ca. 7.8 Hz, *meta*-H NPh_2), 7.15 (d, 4H, J_{HH} 7.8 Hz, *ortho*-H NPh_2), 7.06–7.10 (m, 4H, *para*-H NPh_2 + C_6H_4). Anal. Calc. for $C_{48}H_{32}NP$: C, 88.19; H, 4.93; N, 2.14. Found: C 87.80; H 4.43; N, 2.00.

Synthesis of complexes Au1–Au3. $[Au(epbpy)]_n$ (45.0 mg, 0.1 mmol) and the corresponding phosphine **L1**–**L3** (0.1 mmol) were suspended in degassed dichloromethane (10 ml). The resulting mixture was stirred for 1 h to produce a nearly clear solution, which was passed through a layer of Celite and diluted with an excess of hexanes to precipitate the product. The solid was collected by centrifugation, washed with hexanes (3×5 ml), diethyl ether (3×5 ml) and dried.

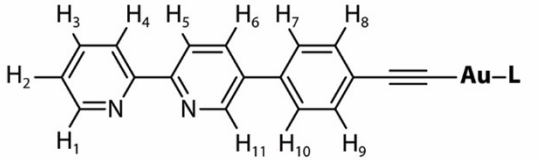

numbering scheme for **Au1**-**Au3**, where **L** = **L1** - **L3**

Au1. Colorless solid (89 mg, 95%). $^{31}P\{^1H\}$ NMR ($CDCl_3$, 298 K; *δ*): 41.7 (s, 1P). ^1H NMR ($CDCl_3$, 298 K; *δ*): 8.94 (d, 1H, J_{HH} 2.2 Hz, 11-H), 8.71 (d, 1H, J_{HH} 4.1, 1.7 Hz; 1-H), 8.44–8.49 (m, 2H, 4,6-H), 8.04 (dd, 1H, J_{HH} 8.1, 2.2 Hz; 5-H), 7.85 (ddd, 1H, J_{HH} 8.0, 7.8, 1.7 Hz; 3-H), 7.70–7.47 (m, 20H, 7,8,9,10-H + $(C_6H_4)_2$ + *ortho*+*meta*+*para*-H PPh_2), 7.35–7.27 (m, 5H, 2-H + *meta*-H NPh_2), 7.13–7.19 (m, 6H, *ortho*-H NPh_2 + $(C_6H_4)_2$), 7.08 (t, 2H, J_{HH} 7.5 Hz, *para*-H NPh_2). Anal. Calc. for $C_{54}H_{39}AuN_3P$: C, 67.71; H, 4.10; N, 4.39. Found: C, 67.62; H, 3.98; N, 4.48.

Au2. Yellow solid (90 mg, 90%). $^{31}P\{^1H\}$ NMR ($CDCl_3$, 298 K; *δ*): 36.8 (s, 1P). ^1H NMR ($CDCl_3$, 298 K; *δ*): 8.93 (d, 1H, J_{HH} 2.0 Hz, 11-H), 8.71 (d, 1H, J_{HH} 4.5, 1.8 Hz; 1-H), 8.56 (d, 1H, J_{HH} 8.3 Hz, naphthalene), 8.52 (d, 1H, J_{HH} 8.7 Hz, naphthalene), 8.43–8.49 (m, 2H, 4,6-H), 8.03 (dd, 1H, J_{HH} 8.2, 2.0 Hz, 5-H), 7.85 (ddd, 1H, J_{HH} ca. 7.8, 1.8 Hz; 3-H), 7.71–7.47 (m, 19H, 7,8,9,10-H + naphthalene + C_6H_4 + *ortho*+*meta*+*para*-H PPh_2), 7.29–7.35 (m, 5H, 2-H+ *meta*-H NPh_2), 7.17 (d, 4H, J_{HH} 8.0 Hz, *ortho*-H NPh_2), 7.11 (t, 2H, J_{HH} 7.3 Hz, *para*-H NPh_2), 7.08 (d, 2H, J_{HH} 8.8,

C_6H_4), 7.01 (dd, 1H, J_{HP} 13.4 Hz, J_{HH} 7.5 Hz, naphthalene). Anal. Calcd for $C_{60}H_{41}AuN_3P$: C, 69.84; H, 4.01; N, 4.07. Found: C, 69.40; H, 4.15; N, 3.93.

Au3. Red solid (92 mg, 86%). $^{31}P\{^1H\}$ NMR ($CDCl_3$, 298 K; δ): 16.5 (s, 1P). ^1H NMR ($CDCl_3$, 298 K; δ): 8.95 (m, 1H, J_{HH} 1.9 Hz, 11-H), 8.76–8.69 (m, 3H, 1-H + anthracene), 8.51–8.42 (m, 4H, 4,6-H + anthracene), 8.10–8.02 (m, 5H, 5-H + *ortho*-H PPh_2), 7.85 (td, 1H, J_{HH} ca. 7.8, 1.7 Hz, 3-H), 7.70–7.55 (m, 16H, 7,8,9,10-H + anthracene + C_6H_4 + *meta*+*para*-H PPh_2), 7.37–7.30 (m, 5H, 2-H + *meta*-H NPh_2), 7.20 (d, 4H, J_{HH} 7.6 Hz, *ortho*-H NPh_2), 7.17–7.10 (m, 4H, *para*-H NPh_2 + C_6H_4). Anal. Calcd for $C_{66}H_{43}AuN_3P$: C, 71.67; H, 3.92; N, 3.80. Found: C, 71.72; H, 4.11; N, 3.46.

Synthesis of complexes Au1Eu–Au3Eu. $Eu(tta)_3\times2H_2O$ (1 eq.) and the corresponding metalloligand **Au1–Au3** (1 eq.) were dissolved in dichloromethane (10 ml). The resulting solution was stirred for 1 h, diluted with hexanes (10 ml) and filtered. Solid residue was dissolved in toluene (5 ml), filtered through a layer of Celite and evaporated. Obtained precipitate was washed with acetone/pentane mixture (3×10 ml, 1/10 v/v), dissolved in toluene (2 ml) and precipitated by adding to a vigorously stirred pentane (20 ml). The solid was collected by centrifugation and dried *in vacuo*.

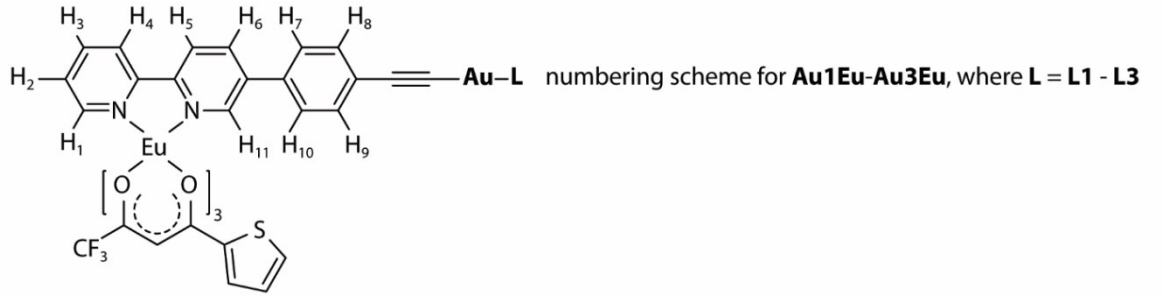

numbering scheme for **Au1Eu-Au3Eu**, where **L** = **L1** - **L3**

Au1Eu. Colorless solid (83 %).$^{31}P\{^1H\}$ NMR ($CDCl_3$, 298 K; δ): 41.6 (s, 1P). ^1H NMR (CD_2Cl_2, 298 K; δ): 14.79 (br s, 1H, 11-H), 14.40 (br s, 1H, 1-H), 9.61–9.80 (m, 4H, 3,4,5,6-H), 8.71–8.82 (m, 3H, 2,8,9-H), 7.89–7.91 (m, 2H, 7,10-H), 7.57–7.80 (m, 16H, $(C_6H_4)_2$ + *ortho*+*meta*+*para*-H PPh_2), 7.33 (dd, 4H, J_{HH} 7.9 Hz, *meta*-H NPh_2), 7.05–7.18 (m, 11H, *ortho*+*para*-H NPh_2 + tta + $(C_6H_4)_2$), 6.54–6.56 (m, 3H, tta), 6.16 (br s, 3H, tta), 2.97 (br s, 3H, tta). FTIR (KBr, cm^{-1}): ν = 2114 (C≡C), 1599 (C=O). Anal. Calc. for $C_{78}H_{51}AuEuF_9N_3O_6PS_3$: C, 52.83; H, 2.90; N, 2.37. Found: C, 53.06; H, 3.04; N, 2.35.

Au2Eu. Yellow solid (78 %). $^{31}P\{^1H\}$ NMR (CD_2Cl_2, 298 K; δ): 36.7 (s, 1P). ^1H NMR (CD_2Cl_2, 298 K; δ): 14.77 (br s, 1H, 11-H), 14.37 (br s, 1H, 1-H), 9.61–9.80 (m, 4H, 3,4,5,6-H), 8.62–8.81 (m, 5H, naphthalene + 2,8,9-H), 7.86–7.87 (m, 2H, 7,10-H), 7.51–7.79 (m, 15H, naphthalene + C_6H_4 + *meta*+*ortho*+*para*-H PPh_2), 7.36 (dd, 4H, J_{HH} 7.8 Hz, *meta*-H NPh_2), 7.04–7.20 (m, 12H, tta + naphthalene + C_6H_4 + *para*+*ortho*-H NPh_2), 6.53–6.55 (m, 3H, tta), 6.15 (br s, 3H, tta), 2.96

(br s, 3H, tta). FTIR (KBr, cm^{-1}): ν = 2197, 2114 (C≡C), 1600 (C=O). Anal. Calc. for $C_{84}H_{53}AuEuF_9N_3O_6PS_3$: C, 54.61; H, 2.89; N, 2.27. Found: C, 54.77; H, 3.01; N, 2.15.

Au3Eu. Red solid (72 %). $^{31}P\{^1H\}$ NMR (CD_2Cl_2, 298 K; δ): 16.3 (s, 1P). ^1H NMR (CD_2Cl_2, 298 K; δ): 14.75 (br s, 1H, 11-H), 14.37 (br s, 1H, 1-H), 9.62–9.84 (m, 4H, 3,4,5,6-H), 8.71–8.79 (m, 5H, 2,8,9-H + anthracene), 8.57 (d, 2H, J_{HH} 8.5 Hz, anthracene), 8.13–8.19 (m, 4H, anthracene), 7.90–7.92 (m, 2H, 7,10-H), 7.62–7.78 (m, 11H, anthracene + *ortho*+*meta*+*para*-H PPh_2), 7.35 (dd, 4H, J_{HH} 7.9 Hz, *meta*-H NPh_2), 7.12–7.22 (m, 12H, *ortho*+*para*-H NPh_2 + C_6H_4 + tta), 6.55 (br s, 3H, tta), 6.15 (br s, 3H, tta), 2.97 (br s, 3H, tta). FTIR (KBr, cm^{-1}): ν = 2182 (C≡C), 2139 (C≡C), 1601 (C=O). Anal. Calc. for $C_{90}H_{55}AuEuF_9N_3O_6PS_3$: C, 56.26; H, 2.89; N, 2.19. Found: C, 55.99; H, 2.98; N, 2.11.

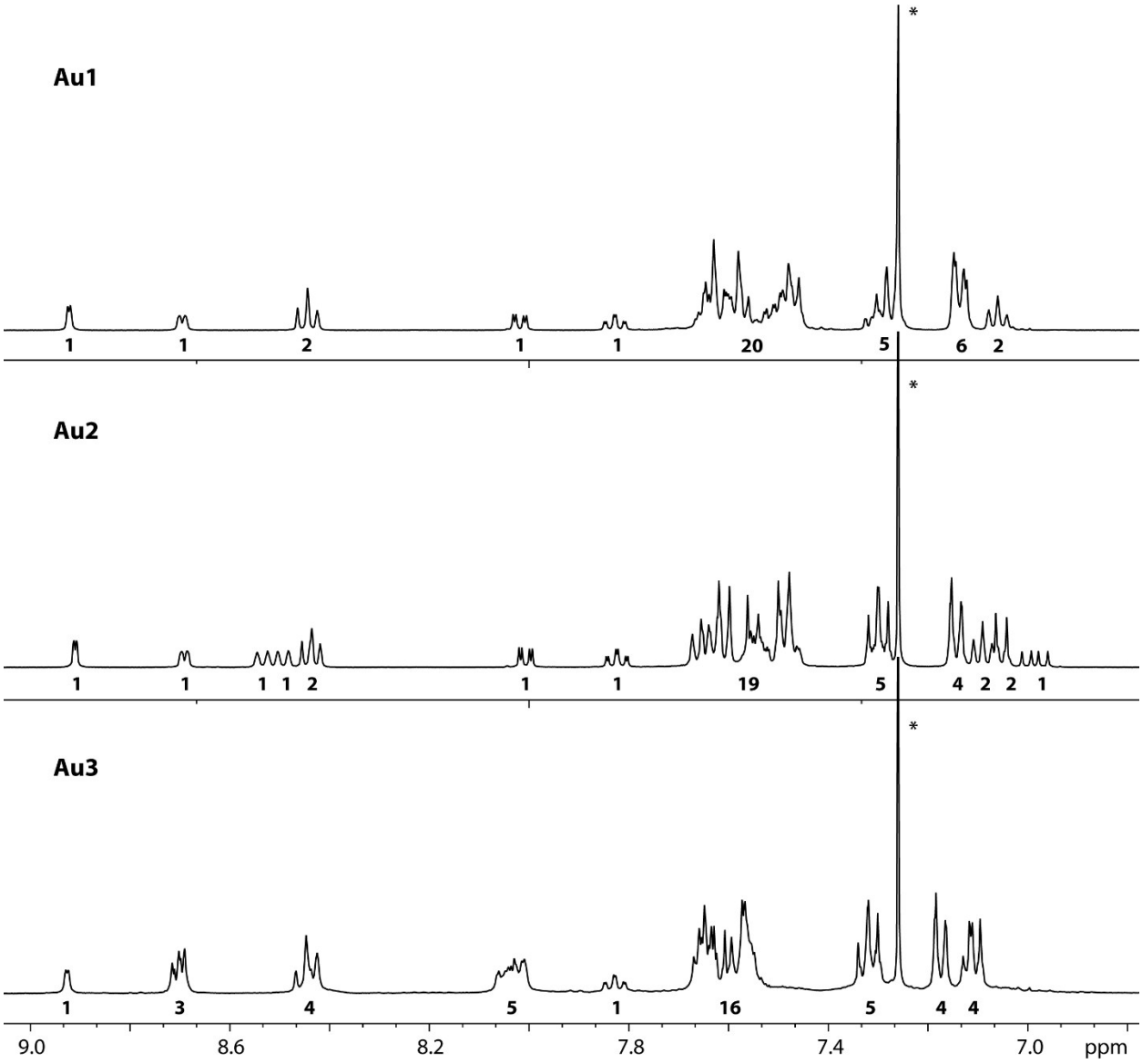

Figure S1. ^1H NMR spectra of **Au1**–**Au3** ($CDCl_3$, 298 K). The numbers under the signals indicate relative integral intensities, * at 7.26 ppm indicates chloroform residual signal.

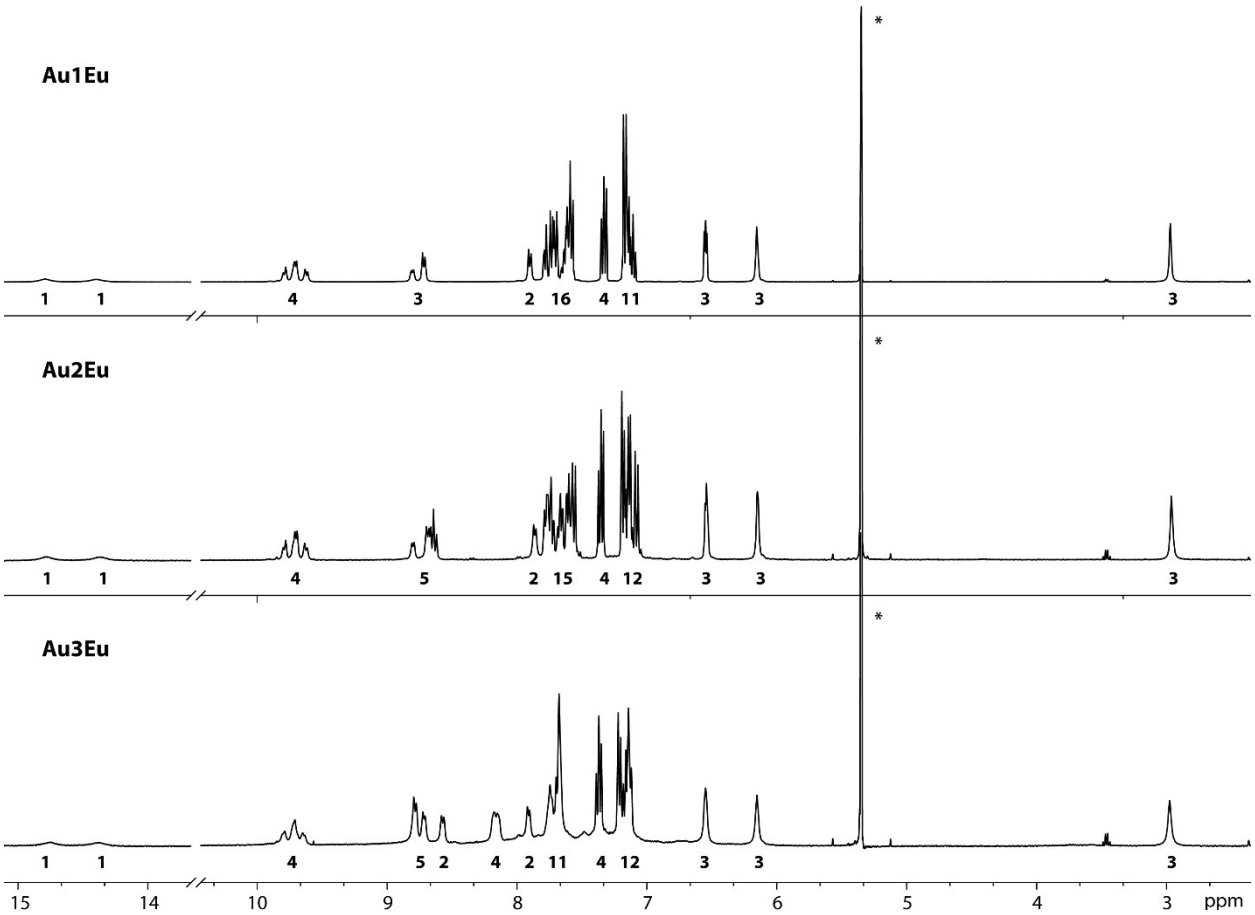

Figure S2. ^{1}H NMR spectra of **Au1Eu**–**Au3Eu** (CD_2Cl_2, 298 K). The numbers under the signals indicate relative integral intensities, * at 5.32 ppm indicates dichloromethane residual signal.

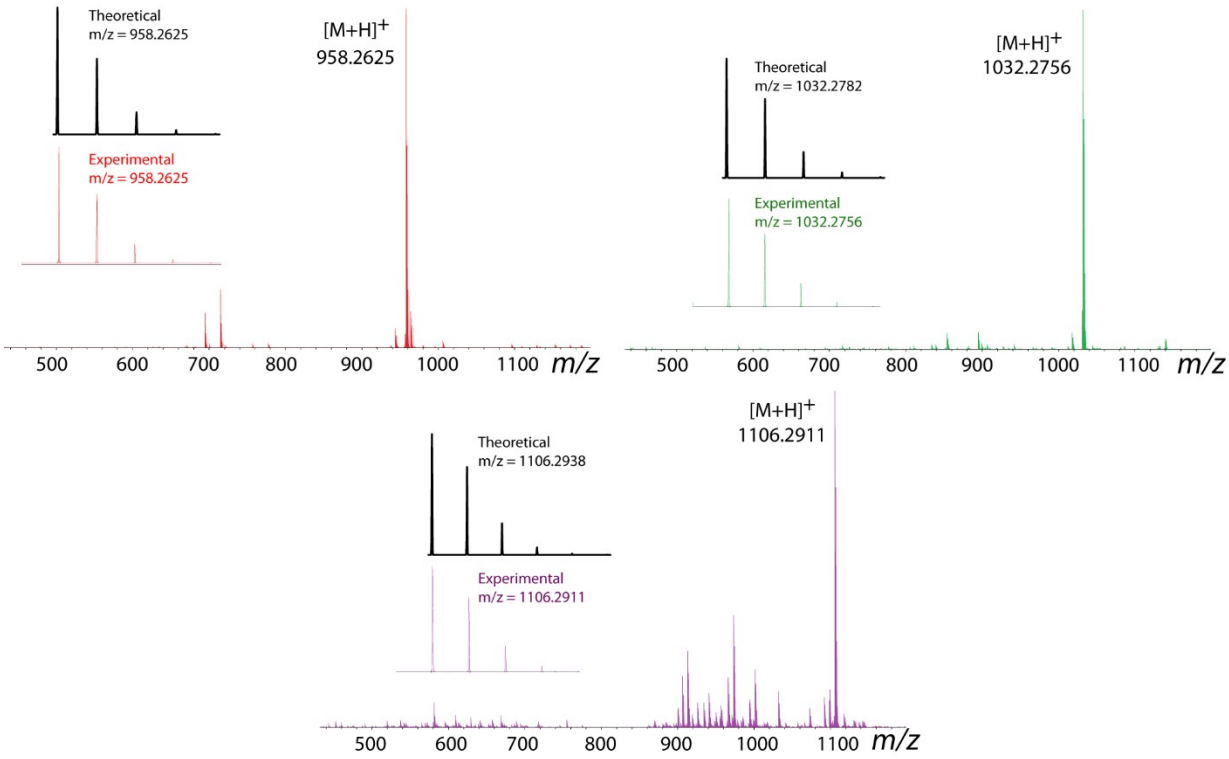

Figure S3. Mass spectra of **Au1**–**Au3** (ESI^+), dichloromethane /methanol.

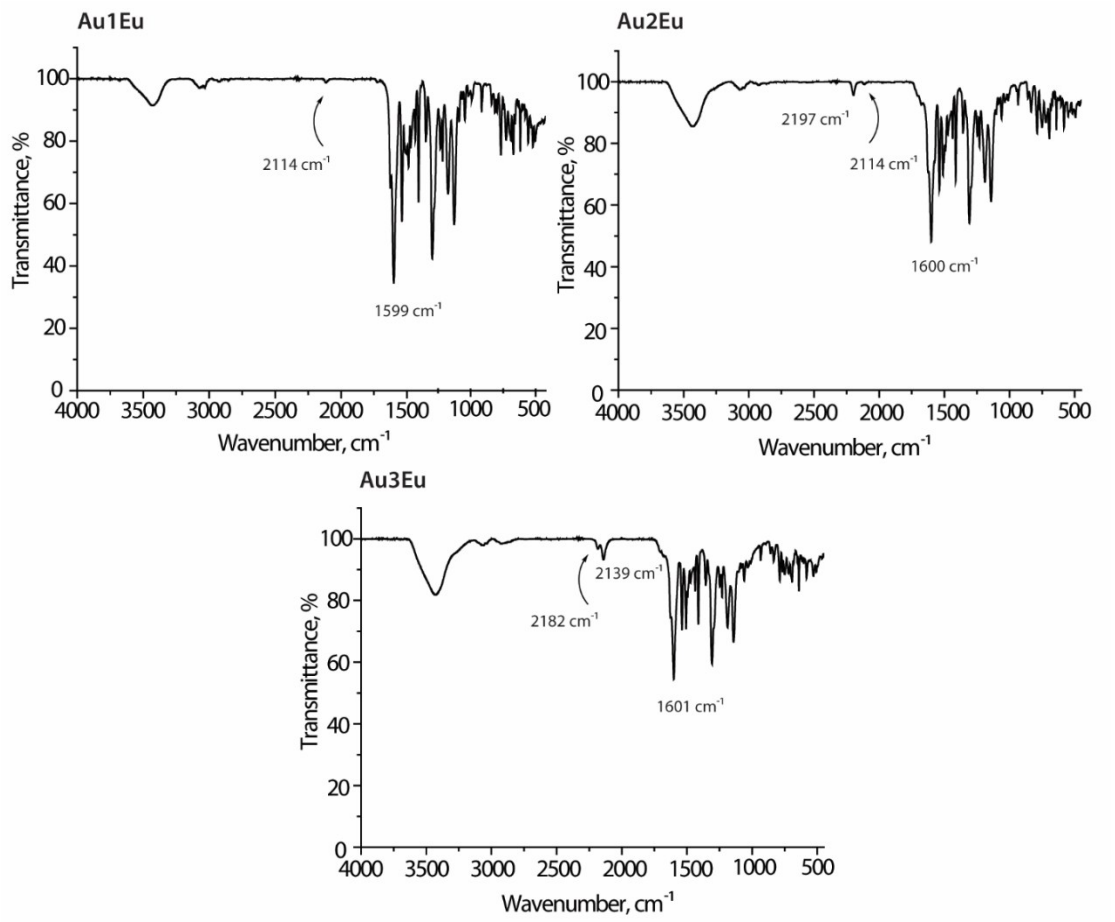

Figure S4. FTIR spectra of **Au1Eu**–**Au3Eu** (KBr).

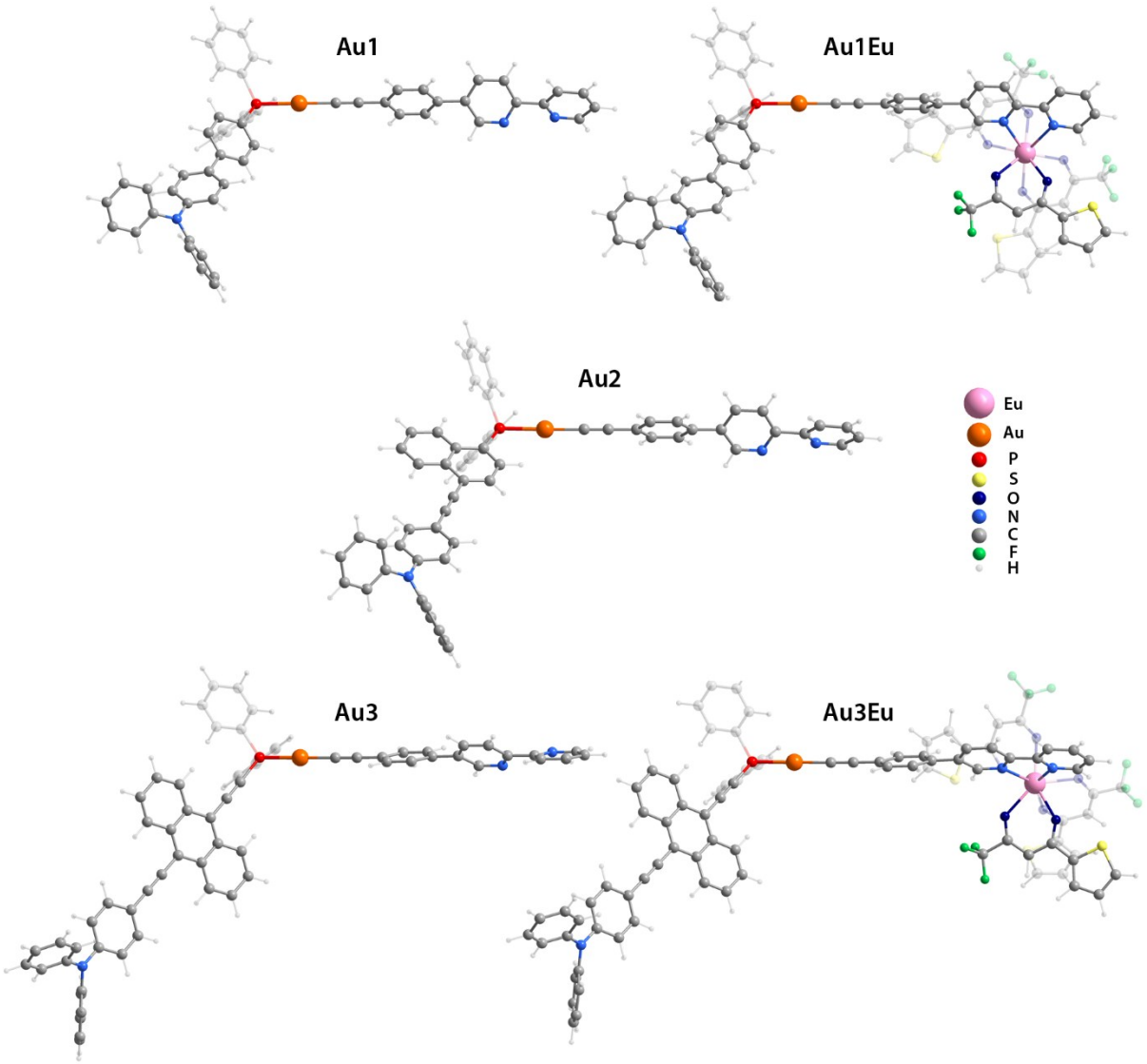

Figure S5. Minimum energy structures of complexes **Au1–Au3** and **Au3Eu**, **Au3Eu** (DFT LC-PBE method).

Table S1. Bond lengths for gold complexes **Au1–Au3** and **Au1Eu–Au3Eu** dyads estimated by geometry optimization.

	Bond lengths, Å			
	Au–P	**Au–C**	**Eu–**	**Eu–N**
Au1	2.284	1.973	–	–
Au2	2.289	1.972	–	–
Au3	2.279	1.971	–	–
Au1Eu	2.284	1.973	2.370	2.586
Au2Eu	2.289	1.972	2.370	2.588
Au3Eu	2.279	1.971	2.369	2.586

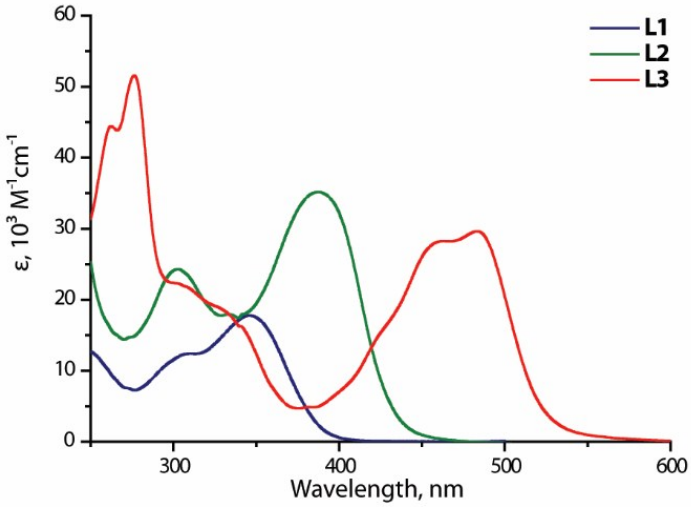

Figure S6. UV-vis absorption spectra of the phosphine ligands **L1**–**L3** in 1,2-dichloroethane.

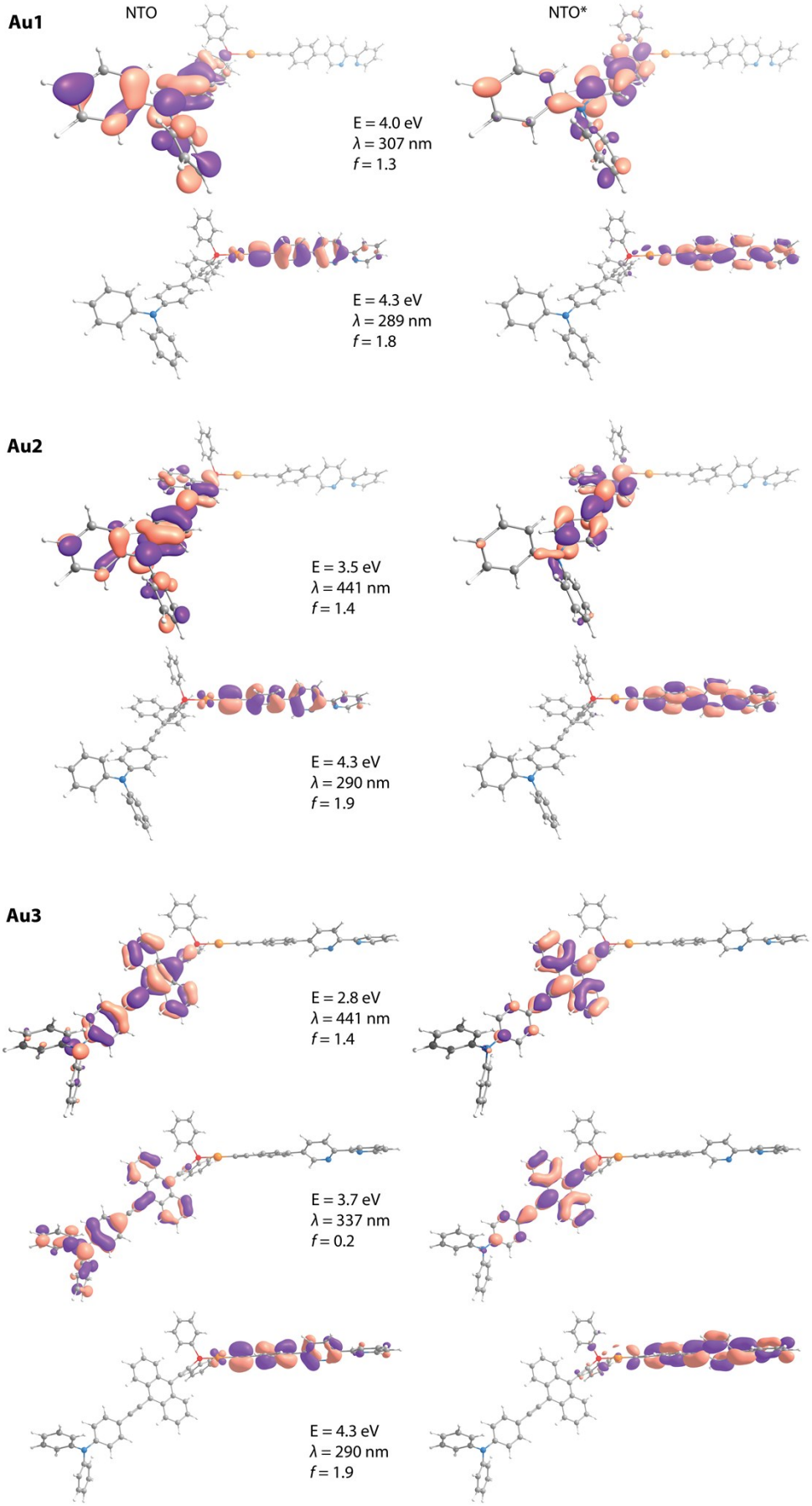

Figure S7. Natural transition orbitals involved in the lowest energy singlet electronic excitations for complexes **Au1–Au3**.

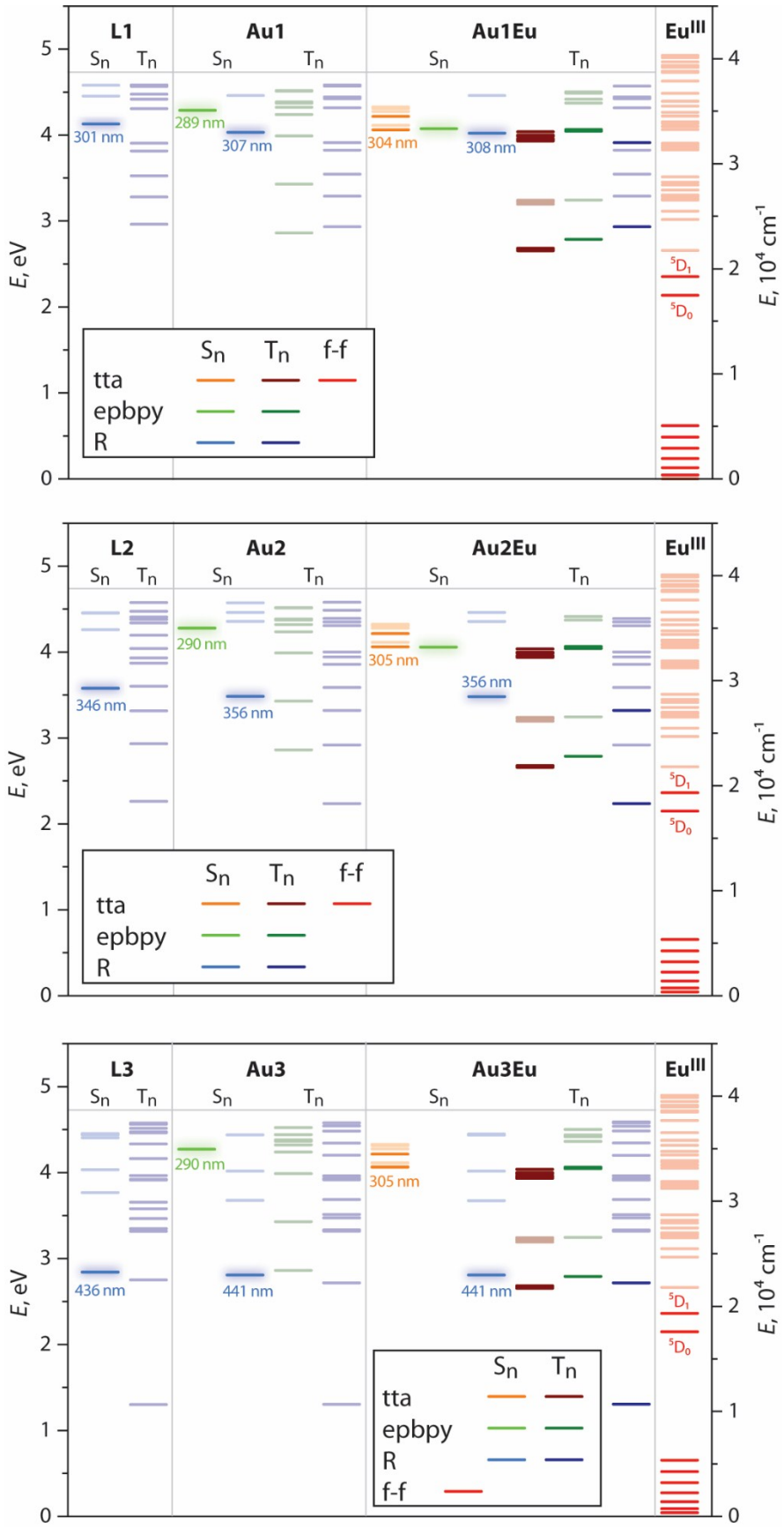

Figure S8. Excited state diagrams for the phosphine ligands **L1**–**L3**, complexes **Au1**–**Au3** and **Au1Eu**–**Au3Eu** predicted by TDDFT analysis. Energy levels of the Eu(III) ion (right) are provided for comparison.[19]

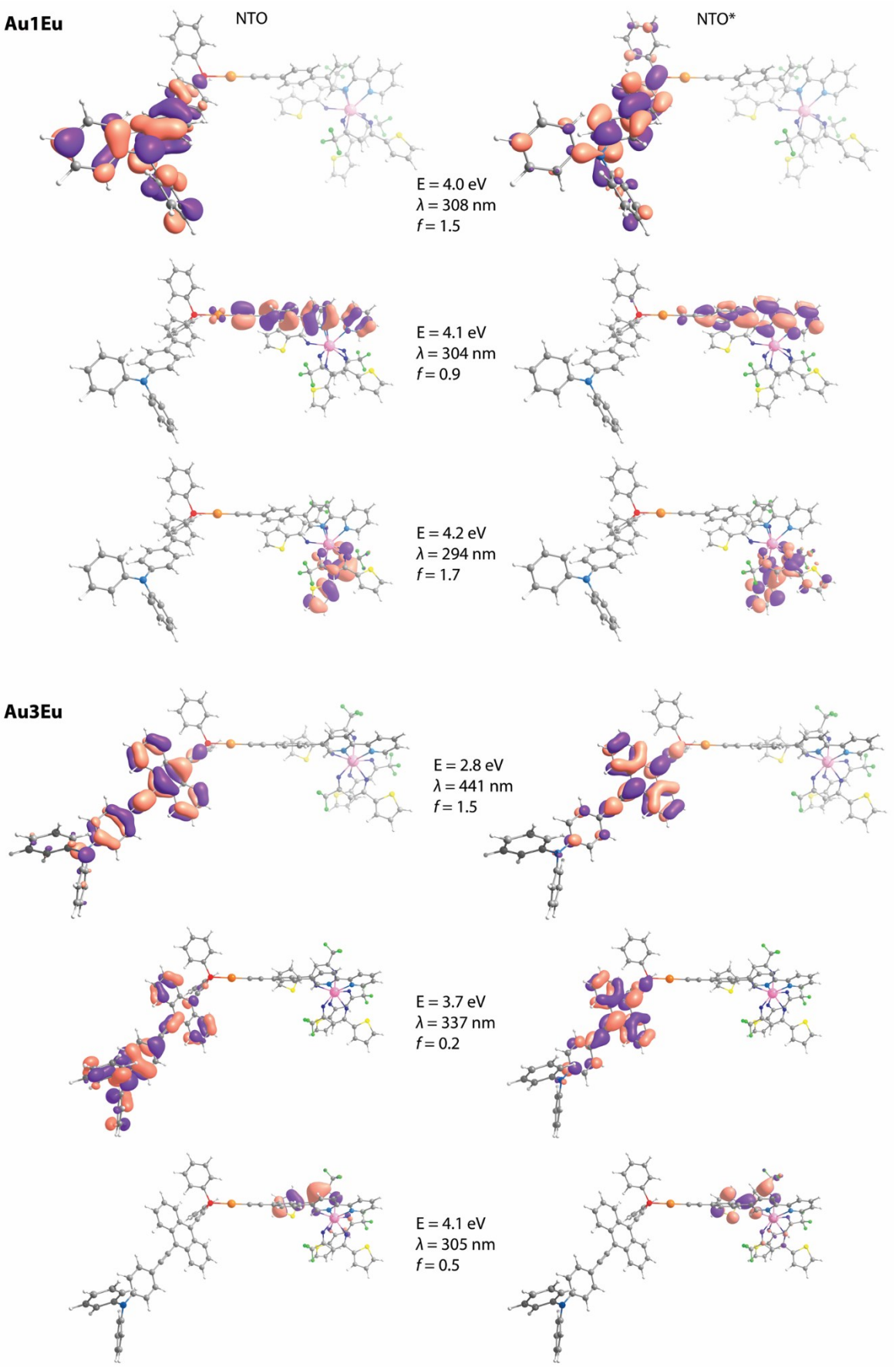

Figure S9. Natural transition orbitals involved in the lowest energy singlet electronic excitations for complexes **Au1Eu** and **Au3Eu**.

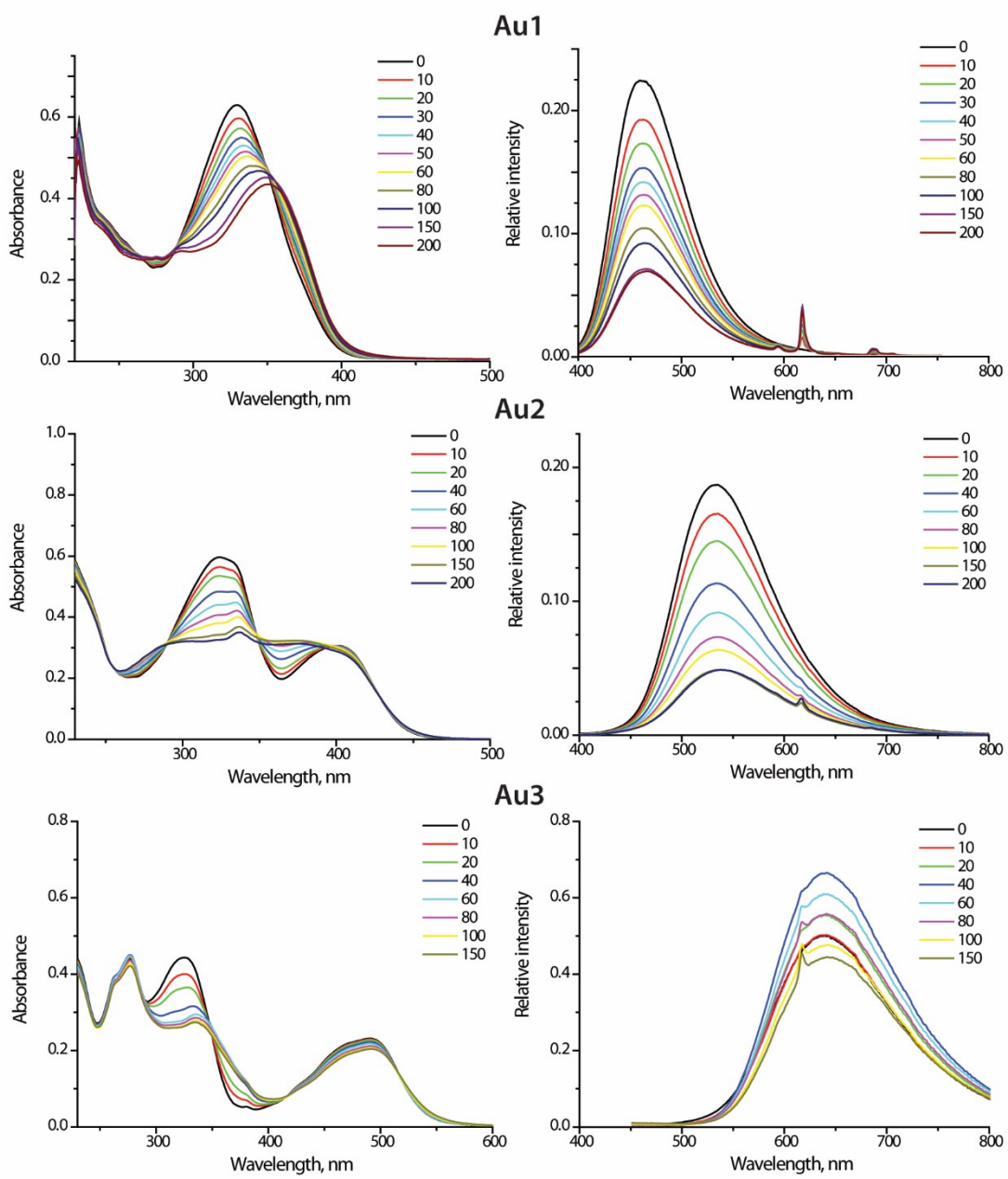

Figure S10. Changes of the absorption (left) and emission (right) spectra of **Au1–Au3** (10^{-5} M DCE solutions) upon titration with $Eu(NO_3)_3$ (10^{-4} M acetonitrile solution).

Table S2. Photophysical characteristics of **Au1**–**Au3** in different solvents at 298 K.

	CHX	Toluene	Et_2O	$CHCl_3$	THF	DCM	Acetone	MeCN
				Au1				
λ_{abs}, nm[a]	334	335	330	327	333	328	334	327
λ_{em}, nm[a,b]	403, 423	425	435	445	450	460	475	490
ν_{St}, cm^{-1}	5126	6321	7315	8109	7808	8748	8887	10173
CIE[c]	0.15, 0.02	0.15, 0.05	0.15, 0.07	0.15, 0.09	0.15, 0.13	0.15, 0.16	0.17, 0.26	0.20, 0.34
				Au2				
λ_{abs}[a]	334, 388	336, 401	332, 393	321, 402	334, 395	321, 400	393	321, 392
λ_{em}[a,b]	428, 450	460	480	495	515	525	560	580
ν_{St}	3550	3198	4612	4673	5899	5952	7588	8269
CIE[c]	0.15, 0.08	0.16, 0.19	0.17, 0.30	0.21, 0.40	0.28, 0.50	0.31, 0.53	0.42, 0.51	0.47, 0.48
				Au3				
λ_{abs}[a]	326, 490	329, 498	325, 487	324, 493	329, 489	326, 492	484	325, 483
λ_{em}[a,b]	520, 555	550	572	590	620	630	644	666
ν_{St}	1177	1898	3051	3334	4321	4452	5133	5689
CIE[c]	0.33, 0.61	0.43, 0.55	0.48, 0.50	0.53, 0.46	0.57, 0.42	0.58, 0.40	0.53, 0.42	0.48, 0.40

[a] measured at 0.15 O.D. at the excitation wavelength; [b] fluorescence band, λ_{exc} = 365 nm; [c] (x, y), calculated from emission spectra.

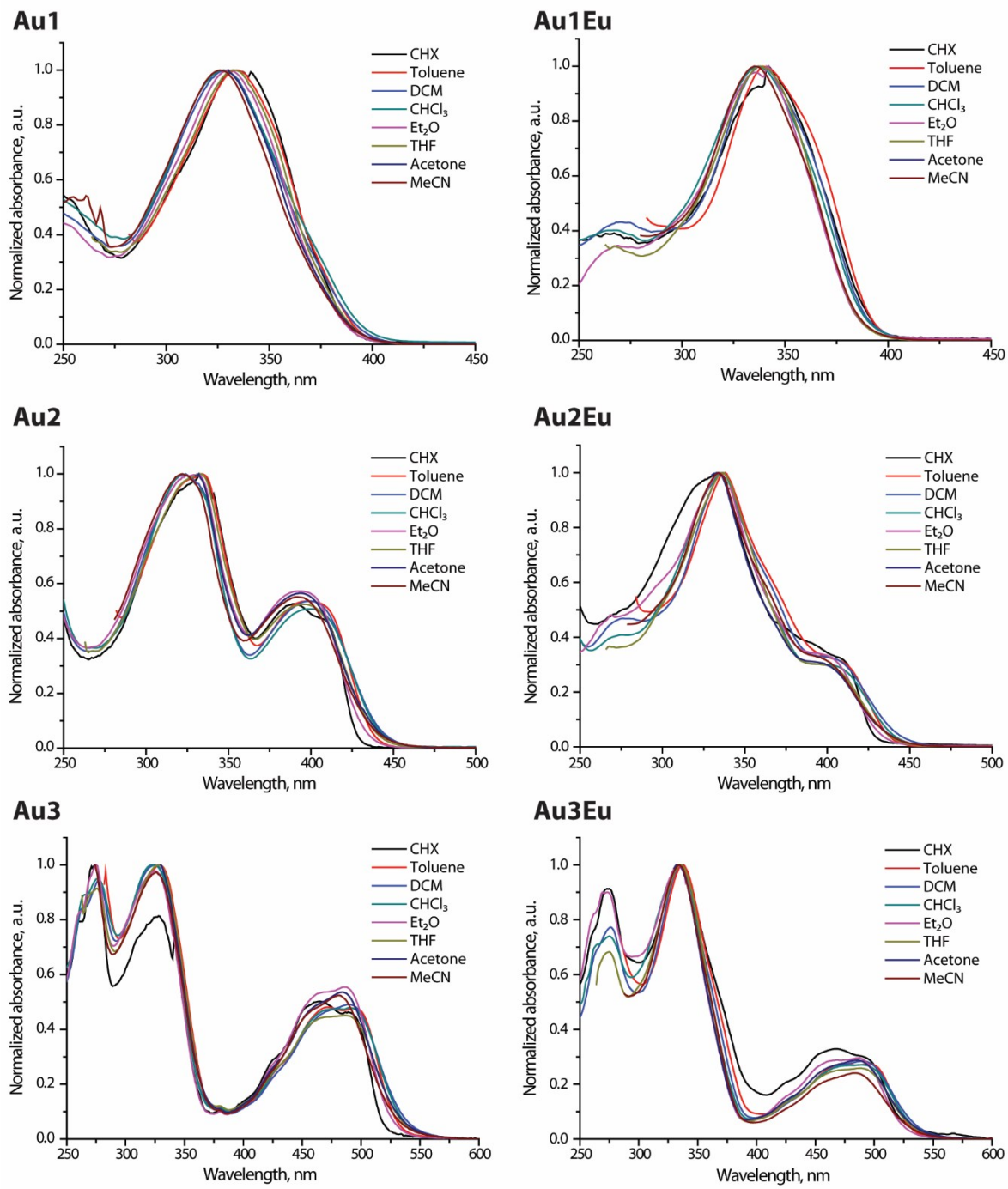

Figure S11. Normalized absorption spectra of **Au1**–**Au3** and **Au1Eu**–**Au3Eu** in solvents with different polarity (cyclohexane CHX, toluene, dichloromethane DCM, chloroform, diethyl ether, tetrahydrofuran THF, acetone, and acetonitrile MeCN).

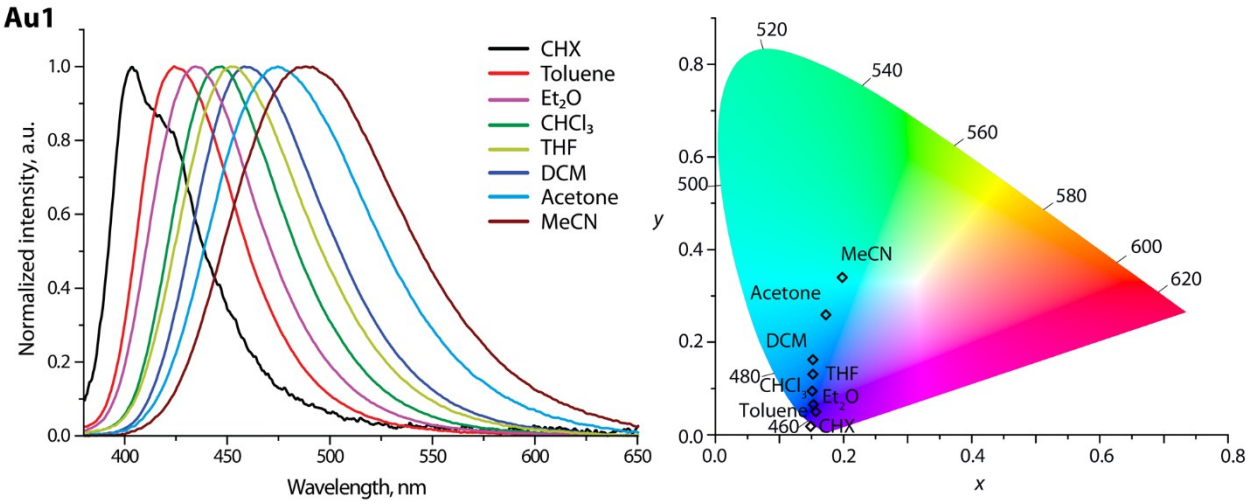

Figure S12. Normalized emission spectra (left, λ_{exc} = 365 nm) and CIE 1931 coordinates (right) for **Au1** in different solvents.

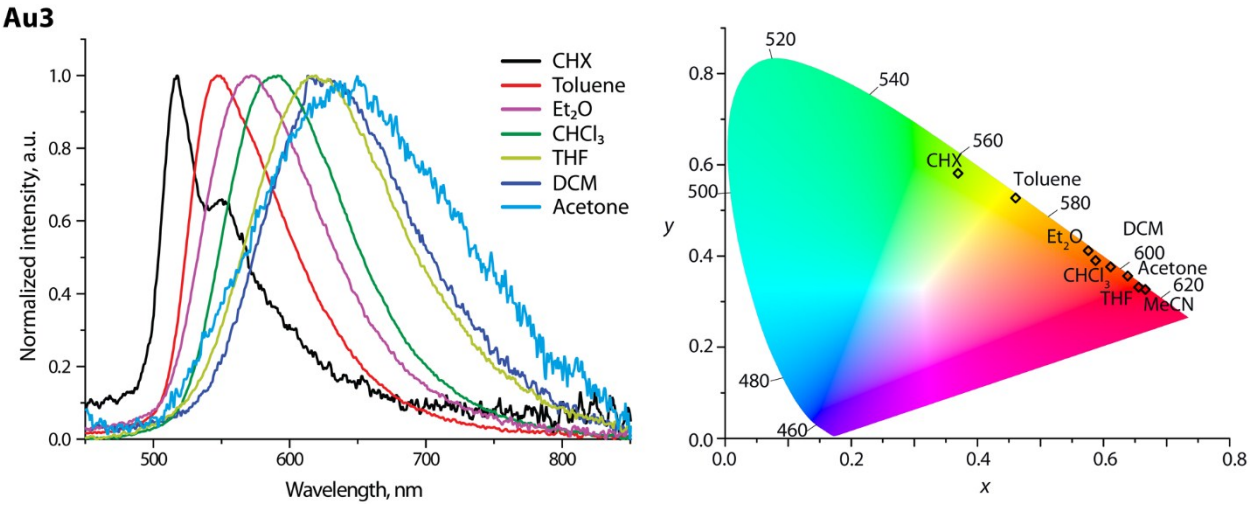

Figure S13. Normalized emission spectra (left, λ_{exc} = 365 nm) and CIE 1931 coordinates (right) for **Au3** in different solvents.

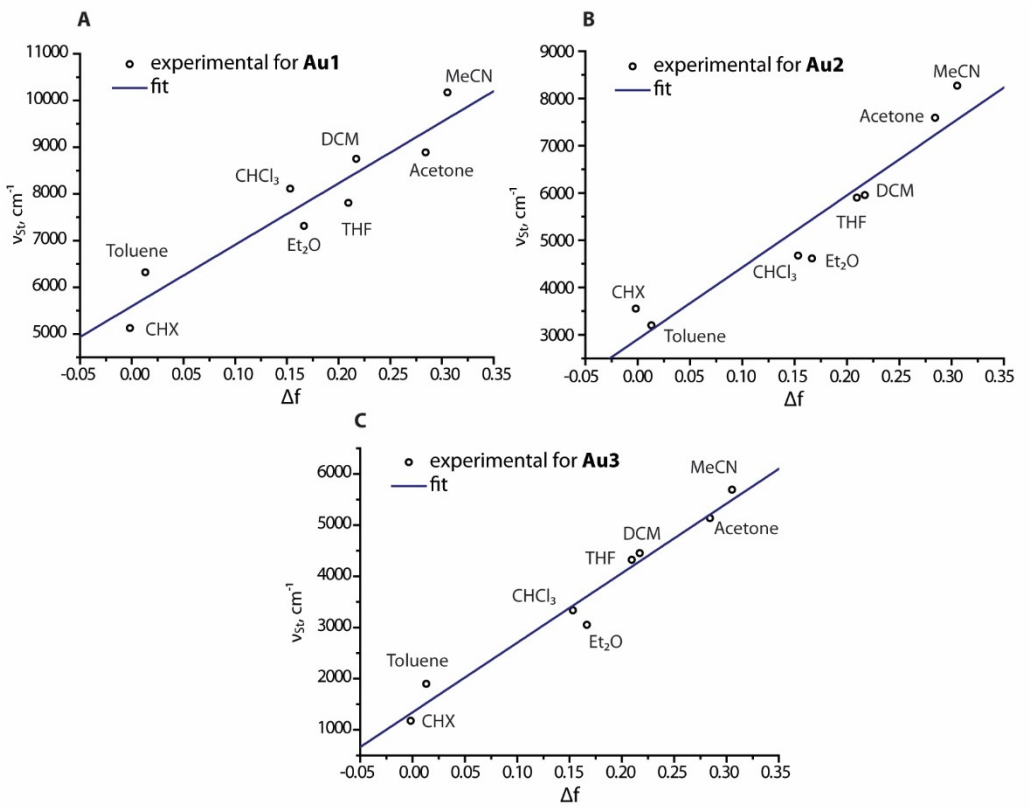

Figure S14. Lippert-Mataga plots $\nu_{St} = k \times \Delta f + b$ of the linear relation between the Stokes shift (ν_{St}) and solvent polarity (Δf, cyclohexane CHX, toluene, dichloromethane DCM, chloroform $CHCl_3$, diethyl ether Et_2O, tetrahydrofuran THF, acetone and acetonitrile MeCN) for compounds (A): **Au1**, slope = 13162±1867, intercept = 5593±371, correlation coefficient R = 0.87; (B): **Au2**, slope = 15224±2026, intercept = 2902±403, correlation coefficient R = 0.89; (C) **Au3**, slope = 13587±1024, intercept = 1342±203, correlation coefficient R = 0.96.

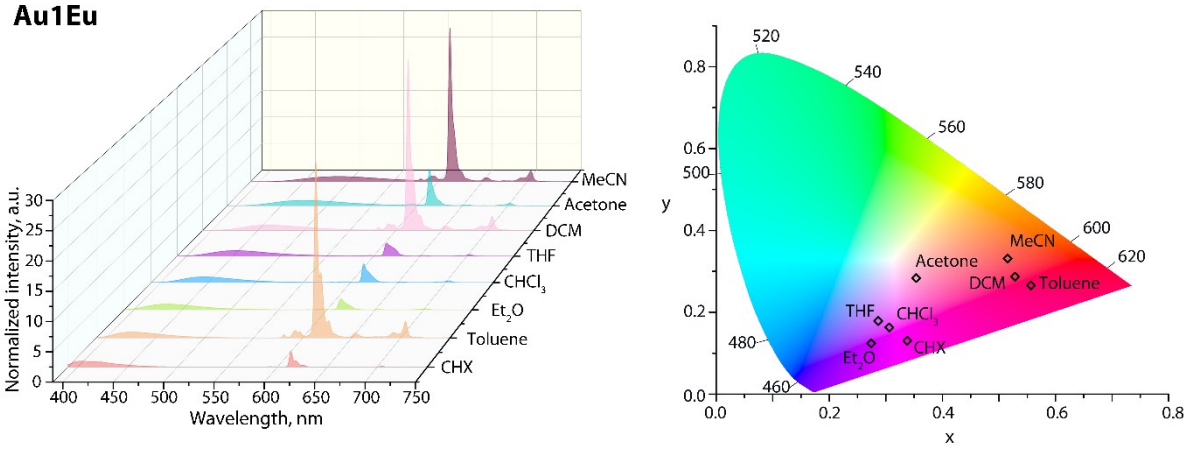

Figure S15. The emission spectra (left, λ_{exc} = 365 nm, normalized on the fluorescence band) and CIE 1931 coordinates (right) for **Au1Eu** in different solvents.

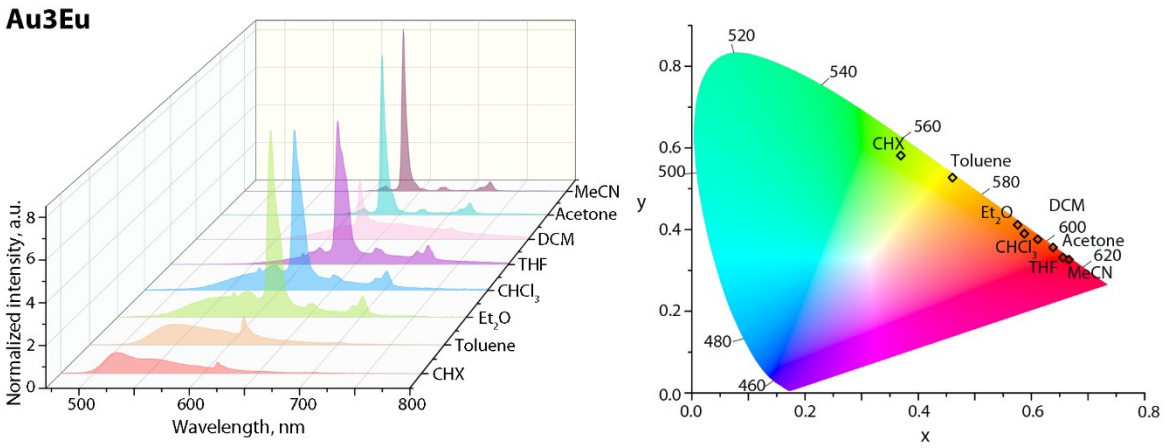

Figure S16. The emission spectra (left, λ_{exc} = 365 nm, normalized on the fluorescence band) and CIE 1931 coordinates (right) for **Au3Eu** in different solvents.

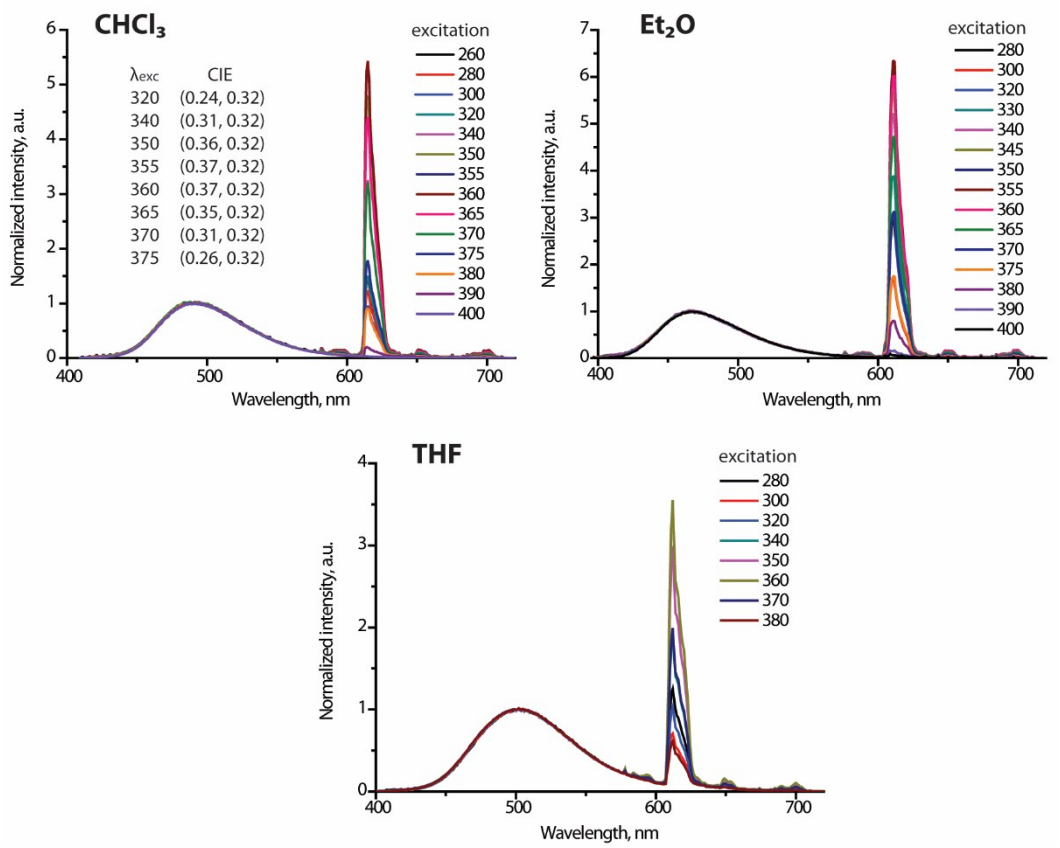

Figure S17. The emission spectra of **Au2Eu** normalized on the fluorescence band at different excitation wavelengths in chloroform ($CHCl_3$), diethyl ether (Et_2O) and tetrahydrofuran (THF).

References

1. Li, Z. H.; Wong, M. S.; Tao, Y.; D'Iorio, M. Synthesis and Functional Properties of Strongly Luminescent Diphenylamino End-Capped Oligophenylenes. *J. Org. Chem.* **2004,** *69*, 921–927.

2. Gao, H.; Li, Y.; Wang, L.; Ji, C.; Wang, Y.; Tian, W.; Yang, X.; Yin, L. High performance asymmetrical push–pull small molecules end-capped with cyanophenyl for solution-processed solar cells. *Chem. Commun.* **2014,** *50*, 10251-10254.

3. Wang, J.; Wan, W.; Jiang, H.; Gao, Y.; Jiang, X.; Lin, H.; Zhao, W.; Hao, J. C-9 Fluorenyl Substituted Anthracenes: A Promising New Family of Blue Luminescent Materials. *Org. Lett.* **2010,** *12*, 3874-3877.

4. Solovjov, I. V.; Kondinski, A.; Monakhov, K. Y.; Koshevoy, I. O.; Grachova, E. V. Synthesis, photophysical properties and cation-binding studies of bipyridine-functionalized gold(I) complexes. *Inorg. Chem. Front.* **2018,** *5*, 160-171.

5. Melby, L. R.; Rose, N. J.; Abramson, E.; Caris, J. C. Synthesis and Fluorescence of Some Trivalent Lanthanide Complexes. *J. Am. Chem. Soc.* **1964,** *86*, 5117-5125.

6. Perdew, J. P.; Burke, K.; Ernzerhof, M. Generalized Gradient Approximation Made Simple. *Phys. Rev. Lett.* **1996,** *77*, 3865-3868.

7. Iikura, H.; Tsuneda, T.; Yanai, T.; Hirao, K. A long-range correction scheme for generalized-gradient-approximation exchange functionals. *J. Chem. Phys.* **2001,** *115*, 3540-3544.

8. Yanai, T.; Tew, D. P.; Handy, N. C. A new hybrid exchange–correlation functional using the Coulomb-attenuating method (CAM-B3LYP). *Chem. Phys. Lett.* **2004,** *393*, 51-57.

9. Dolg, M.; Stoll, H.; Savin, A.; Preuss, H. Energy-adjusted pseudopotentials for the rare earth elements. *Theoret. Chim. Acta* **1989,** *75*, 173-194.

10. Mennucci, B.; Cancès, E.; Tomasi, J. Evaluation of Solvent Effects in Isotropic and Anisotropic Dielectrics and in Ionic Solutions with a Unified Integral Equation Method: Theoretical Bases, Computational Implementation, and Numerical Applications. *J. Phys. Chem. B* **1997,** *101*, 10506-10517.

11. Cancès, E.; Mennucci, B.; Tomasi, J. A new integral equation formalism for the polarizable continuum model: Theoretical background and applications to isotropic and anisotropic dielectrics. *J. Chem. Phys.* **1997,** *107*, 3032-3041.

12. Improta, R.; Barone, V.; Scalmani, G.; Frisch, M. J. A state-specific polarizable continuum model time dependent density functional theory method for excited state calculations in solution. *J. Chem. Phys.* **2006,** *125*, 054103.

13. Martin, R. L. Natural transition orbitals. *J. Chem. Phys.* **2003,** *118*, 4775-4777.

14. Frisch, M. J.; Trucks, G. W.; Schlegel, H. B.; Scuseria, G. E.; Robb, M. A.; Cheeseman, J. R.; Scalmani, G.; Barone, V.; Petersson, G. A.; Nakatsuji, H.; Li, X.; Caricato, M.; Marenich, A. V.; Bloino, J.; Janesko, B. G.; Gomperts, R.; Mennucci, B.; Hratchian, H. P.; Ortiz, J. V.; Izmaylov, A. F.; Sonnenberg, J. L.; Williams-Young, D.; Ding, F.; Lipparini, F.; Egidi, F.; Goings, J.; Peng, B.; Petrone, A.; Henderson, T.; Ranasinghe, D.; Zakrzewski, V. G.; Gao, J.; Rega, N.; Zheng, G.; Liang, W.; Hada, M.; Ehara, M.; Toyota, K.; Fukuda, R.; Hasegawa, J.; Ishida, M.; Nakajima, T.; Honda, Y.; Kitao, O.; Nakai, H.; Vreven, T.; Throssell, K.; Montgomery, J. A. J.; Peralta, J. E.; Ogliaro, F.; Bearpark, M. J.; Heyd, J. J.; Brothers, E. N.; Kudin, K. N.; Staroverov, V. N.; Keith, T. A.; Kobayashi, R.; Normand, J.; Raghavachari, K.; Rendell, A. P.; Burant, J. C.; Iyengar, S. S.; Tomasi, J.; Cossi, M.; Millam, J. M.; Klene, M.; Adamo, C.; Cammi, R.; Ochterski, J. W.; Martin, R. L.; Morokuma, K.; Farkas, O.; Foresman, J. B.; Fox, D. J. *Gaussian 16*, Revision A.03; Gaussian, Inc.: Wallingford CT, 2016.

15. Brouwer, A. M. Standards for photoluminescence quantum yield measurements in solution (IUPAC Technical Report). *Pure & Appl. Chem.* **2011,** *83*, 2213–2228.

16. Maus, M.; Rettig, W.; Bonafoux, D.; Lapouyade, R. Photoinduced Intramolecular Charge Transfer in a Series of Differently Twisted Donor-Acceptor Biphenyls As Revealed by Fluorescence. *J. Phys. Chem. A* **1999,** *103*, 3388-3401.

17. Sakuda, E.; Ando, Y.; Ito, A.; Kitamura, N. Extremely Large Dipole Moment in the Excited Singlet State of Tris{[p-(N,N-dimethylamino)phenylethynyl]duryl}borane. *J. Phys. Chem. A* **2010,** *114*, 9144–9150.

18. Yang, X.; Yan, X.; Guo, H.; Liu, B.; Zhao, J.; Zhou, G.; Wu, Y.; Wu, Z.; Wong, W.-Y. Charged dinuclear Cu(I) complexes for solution-processed single-emitter warm white organic light-emitting devices. *Dyes Pigments* **2017,** *143*, 151-164.

19. Carnall, W. T.; Goodman, G. L.; Rajnak, K.; Rana, R. S. A systematic analysis of the spectra of the lanthanides doped into single crystal LaF_3. *J. Chem. Phys.* **1989,** *90*, 3443-3457.